IC/80/142

INTERNATIONAL CENTRE FOR THEORETICAL PHYSICS

ELECTRONIC STRUCTURE OF DISORDERED ALLOYS - I: SELF-CONSISTENT CLUSTER CPA INCORPORATING OFF-DIAGONAL DISORDER AND SHORT-RANGE ORDER

Vijay Kumar

Abhijit Mookerjee

and

V.K. Srivastava

INTERNATIONAL ATOMIC ENERGY AGENCY

UNITED NATIONS EDUCATIONAL, SCIENTIFIC AND CULTURAL ORGANIZATION

1980 MIRAMARE-TRIESTE

IC/80/142

International Atomic Energy Agency
and
United Nations Educational Scientific and Cultural Organization

INTERNATIONAL CENTRE FOR THEORETICAL PHYSICS

ELECTRONIC STRUCTURE OF DISORDERED ALLOYS - I: SELF-CONSISTENT CLUSTER CPA INCORPORATING OFF-DIAGONAL DISORDER AND SHORT-RANGE ORDER *

Vijay Kumar * Abhijit Mookerjee **
International Centre for Theoretical Physics, Trieste, Italy,

and

V.K. Srivastava
Department of Physics, Indian Institute of Technology, Kanpur, India.

ABSTRACT

We have developed here a self-consistent coherent potential approximation generalized to take into account effect of clusters. Off-diagonal disorder and short-range order are taken into account. A graphical method married to the recursion technique, enables us to work on realistic three-dimensional lattices. Calculations are shown for a binary alloy on a diamond lattice.

MIRAMARE - TRIESTE
September 1980

* To be submitted for publication.

** Present address: Institut für Theoretische Physik, FU, Arnimallee 3, 1000 Berlin 33, Federal Republic of Germany.

*** Permanent address: Department of Physics, Indian Institute of Technology, Kanpur 208016, India.

I. INTRODUCTION

From the real space or the tight-binding viewpoint of the study of electronic states in random alloys, the need to go beyond the single site coherent potential approximation has been felt for a long time. Not only are the effects of random clustering often important, especially in the impurity band of alloys whose constituent core potentials are very dissimilar, but incorporation of off-diagonal disorder inherent in any realistic model, and short-range order due to chemical clustering tendencies necessitates the extension of the single site to cluster CP approximation.

Time to time suggestions have been put forward about ways of generalizing the CPA and ways of incorporating off-diagonal disorder and short-range order. A comprehensive account of these suggestions have been disqussed by Kumar and Joshi (1979) and Mookerjee (1979). Calculations based on these attempts suffer from three main drawbacks. Firstly, the exhaustive "correct" formulations are seemingly intractable as far as actual realistic calculations go. Secondly, there seems to be ambiguity about ways of generalizing the 1CPA. Finally, and most seriously, any tractable, in other words further simplified approximations always lead to unphysical averaged Green functions in the strong scattering regime. The essential herglotz property is violated.

Basing ourselves on the augmented space formalism introduced by one of us (Mookerjee 1973) we present here an unambigious, tractable generalization of the 1CPA which retains the herglotz property for all range of disorder. Off-diagonal disorder and short-range order have been incorporated.

Recently, there has been a renewed interest in using the augmented space formalism, and its invaluable contribution in generating unambiguous and tractable physical generalizations of the 1CPA have been recognized. In a series of papers (Kaplan and Gray 1976, 1977; Diehl and Leath 1979a,b; Kaplan et al. 1980) the authors have examined the augmented space formalism and have generated self-consistent results with off-diagonal disorder on linear chains in particular (Kaplan et al. 1980). There is a closed and exact relationship of their algebraic equations to the graphical method we wish to adopt. The graphical technique has the added advantage that it is ideally suited, in conjunction with the recursion technique of Haydock et al. (1972), for application to realistic models on three-dimensional lattices. The equivalent algebraic equations soon become tediously unwieldy as soon as the cluster size increases, particularly on a three-dimensional lattice. This is the principal contribution of this work and an indicator of its future usefulness.

We present here self-consistent cluster calculations of a single orbital model on the diamond lattice. In a future contribution .(Mookerjee and Chaudhry 1980) we shall apply the ideas on a chemical pseudopotential model for a series of III-V ternary alloys (e.g. $Ga_xIn_{1-x}As$). The underlying lattice structure is also a diamond lattice, and our basis are pseudowave functions generated from the pseudopotential equation of Anderson (1969) and Bullett (1975) starting from the hybridized sp^3 orbitals. Since the electronic structure of these alloys is of considerable interest, our formalism will provide a powerful tool for reasonably realistic,first-principles theoretical understanding.

II. THE FORMALISM

The augmented space formalism has been described earlier in great detail (Mookerjee 1973); Kaplan and Gray 1976, 1977 and Mookerjee 1979). A brief note is however essential before we discuss the cluster generalizations. The starting Hamiltonian is a tight-binding type:

$$\underline{H} = \sum_i \sum_n e_{in} \underline{P}_{in} + \sum_{i \neq j} \sum_n \sum_m V_{in,jm} \underline{T}_{in,jm} \qquad \underline{H} \in \mathcal{H} \quad , \qquad (1)$$

where $\underline{P}$ and $\underline{T}$ are projection operators and transfer operators in $\mathcal{H}$; n,m are band or orbital indices. Both the diagonal terms $\{e_{in}\}$ and the off-diagonal terms $\{V_{in,jm}\}$ form a set of random variables described by

$$e_{in} = e_{in}^A N_i + e_{in}^B (1-N_i)$$

$$V_{in,jm} = V_{nm}^{AA} N_i N_j + V_{nm}^{BB} (1-N_i)(1-N_j) + V_{nm}^{AB} N_i(1-N_j) + N_j(1-N_i) \quad , \qquad (2a)$$

where $\{N_i\}$ are a set of random "occupation" variables for the solute A in the solvent B. In the absence of short-range order the various N_i's are independent random variables with probability densities

$$p(N_i) = c\,\delta(N_i - 1) + (1-c)\,\delta(N_i) \quad . \qquad (2b)$$

Using (2a) we may rewrite (1) in a more useful form

$$\underline{H} = \underline{H}_B + \sum_i \sum_n e_n N_i \underline{P}_{in} + \sum_{i \neq j} \sum_n \sum_m V_{nm}^{(1)} N_i N_j \underline{T}_{in,jm} + \sum_{i \neq j} \sum_n \sum_m V_{nm}^{(2)} (N_i + N_j) \underline{T}_{in,jm} \quad , \qquad (3)$$

where $\underline{H}_B$ is the Hamiltonian of the pure solvent, $e_n = e_n^A - e_n^B$ $V_{nm}^{(1)} = V_{nm}^{AA} + V_{nm}^{BB} - 2V_{nm}^{AB}$ and $V_{nm}^{(2)} = V_{nm}^{AB} - V_{nm}^{BB}$.

The Hamiltonian is now in a form appropriate for the augmented space formalism. Corresponding to each N_i there is a operator $\underline{M}^{(i)}$ in a two-dimensional vector space $\phi^{(i)}$. A representation of $\underline{M}^{(i)}$ in a basis $(|v_0^i\rangle , |v_1^i\rangle)$ is

$$\begin{pmatrix} c & \{c(1-c)\}^{\frac{1}{2}} \\ \{c(1-c)\}^{\frac{1}{2}} & 1-c \end{pmatrix} \qquad \text{(Mookerjee 1973)} \quad ,$$

where c is the concentration of the solute A. The augmented space Hamiltonian is

$$\tilde{\underline{H}} = \underline{H}_B \otimes \underline{I} + \sum_n e_n \sum_i \underline{P}_{in} \otimes \underline{M}^{(i)} \otimes \underline{I}^{(i)} + \sum_n \sum_m V_{nm}^{(1)} \sum_{i \neq j} \underline{T}_{in,jm} \otimes \underline{M}^{(i)} \otimes \underline{M}^{(j)} \otimes \underline{I}^{(ij)} + \sum_n \sum_m V_{nm}^{(2)} \sum_{i \neq j} \underline{T}_{in,jm} \otimes (\underline{M}^{(i)} \otimes \underline{I}^{(i)} + \underline{M}^{(j)} \otimes \underline{I}^{(j)})$$

$$\tilde{\underline{H}} \in \mathcal{H} \otimes \prod \otimes \phi^{(i)} \qquad (4)$$

$\underline{I}^{(i)}$, $\underline{I}^{(ij)}$ in the above equation indicates identity operators in all sub-spaces $\phi^{(k)}$ except those superscripted.

The configurationally averaged Green function is then given by

$$\ll G_{in,jm}(z) \gg = \langle \underline{r}_i, n, \tau^o | (z\tilde{\underline{I}} - \tilde{\underline{H}})^{-1} | \underline{r}_j, m, \tau^o \rangle \qquad (5)$$

with $|\tau^o\rangle \equiv \prod_i^{\otimes} |v_0^i\rangle$. Note that to this stage the relations are all exact .

The density of states then follows directly:

$$\ll n(E) \gg = -(1/\pi) \sum_n \mathrm{Im} \ll G_{in,in}(E+i\delta) \gg \quad \delta \to 0^+ \quad . \tag{6}$$

In the language of Kaplan et al.(1980), it is the off-diagonal terms of $\underline{M}^{(i)}$s which are responsible for the creation of pseudofermions or configuration fluctuations above the augmented space "ground state" $|\tau^0\rangle$. In the presence of off-diagonal disorder pseudofermions are simultaneously created at two sites $\underline{r}_i$ and $\underline{r}_j$ by the term $\underline{M}^i \otimes \underline{M}^j$.

Short-range chemical ordering may be described in an elementary way by a Markovian pair type - between neighbouring sites $\underline{r}_i$ and $\underline{r}_j$

$$\begin{aligned} p(N_j;N_i=1) &= \{1-\alpha(1-c)\}\ \delta(N_j-1) + \alpha(1-c)\ \delta(N_j) \\ p(N_j;N_i=0) &= \alpha c\ \delta(N_j-1) + (1-\alpha c)\ \delta(N_j) \end{aligned} \tag{7}$$

The single parameter α then is a measure of short-range ordering. If $\alpha = 1$ then there is no short-range order and the alloy is purely random. If $1 < \alpha < (1-c)^{-1}$, then AB type of clustering is favoured. The maximum value corresponds to a situation when the alloy is not really random at all, but forms a superlattice of A and B constituents. If $\alpha > 1$, then AA or BB type of clustering is favoured.

This type of description of short-range order may be rather crude. Here we are dealing with a "quenched" short-range order, that is, a short-range order that is not governed by thermodynamics and is consequently temperature independent. In more realistic situations one has to go through a more sophisticated formulation involving concentration-concentration fluctuations.

Having formally performed the configuration averaging exactly, we shall now proceed to generate the approximations methodically, keeping in mind the important herglotz property which must not be violated at any stage. We shall adopt a graphical formulation. It is well known that calculation of Green functions on connected graphs, using the nested path technique always produces herglotz results (Haydock 1972, thesis). This methodology has been described in great detail by Bishop and Mookerjee (1974) and Mookerjee (1975a,b).

The graphs are generated as follows:

(a) To each group of members of the basis $|\underline{r}_i,n,\tau^k\rangle$ in augmented space associate a vertex $(i,\tau) \equiv \lambda$. For $n > 1$, it is a vector vertex.

(b) To each pair of vectors $|\underline{r}_i,n,\tau\rangle$ $n = 1,2,\ldots$; $|\underline{r}_j,m,\tau'\rangle$ $m = 1,2,\ldots$ associate a link $(i\tau, j\tau') \equiv (\lambda,\mu)$.

(c) Contribution of a vertex is defined as $k(i,\tau') = R_{nm} = (z\underline{\underline{I}}-\tilde{H}_{in\tau,im\tau})^{-1}$.

(d) Contribution of a link $(i\tau,j\tau')$ is $k(i\tau,j\tau') = L_{nm} = \tilde{H}_{in\tau,jm\tau'}$.

(e) A path is a connected series of vertices and links $(\lambda,\lambda\mu,\mu\ldots\nu\xi,\xi) \equiv P_L$ L is called the length of the path.

(f) Contribution of a path P_L: $\underline{k}(P_L) = \underline{R}^{\lambda}\cdot\underline{L}^{\mu\nu}\cdot\underline{R}^{\mu}\cdot\underline{L}^{\mu\rho}\ldots$

We then have the result

$$\ll G_{in,im}(z) \gg = \sum_{L=0}^{\infty} \sum_{P_L \in C_L} k_{nm}(P_L) \quad , \tag{8}$$

where P_L is a self-avoiding path beginning and ending at the site $\underline{r}_i$ and of length L, and C_L is the collection of all such paths on a given lattice.

The approximation now involves ignoring or delinking the contribution of possible self-avoiding paths. The relation of these polygonal paths to the CPA has been discussed by Bishop and Mookerjee (1974) and Mookerjee (1975b) has demonstrated their relation to the multiple scattering diagrams. The philosophy of approximation is as follows.

We consider exactly all paths that involve only the spatial part of the augmented space, i.e. $\mathscr{H}$. Such paths are connected to the lattice structure and must not be approximated or delinked without destroying some of the features of the underlying lattice. In three and two dimensions the recursion method helps us to deal with this infinite set of paths.

If we want a CCPA with $(\underline{r}_1,\underline{r}_2,\ldots,\underline{r}_N)$ within the cluster, then all polygonal paths that do not completely lie in the subspace $\mathscr{H}$ and involve these vertices and none others must also be exactly accounted for. These are related to the multiple scattering within the cluster.

Larger polygonal paths which involve sites within and without the cluster but which do not completely lie in the subspace $\mathscr{H}$ must be delinked. The type of delinking depends very much on the environment we wish to immerse our cluster in. Immersion in a VCA medium yields the travelling pseudofermion

approximation (generalization of the ATA) of Diehl et al. (1979a). If we wish to immerse in a 1CPA medium, we simply delink all these larger polygonal paths into a Cayley tree (Bishop and Mookerjee). The result is not self consistent and in particular the band width is the same as that of the 1CPA. If we wish to embed our cluster in a self-consistent cluster medium, we partition the lattice in Tsukada type clusters, delink the environment itself into cluster paths and self-consistently calculate the effect. We shall describe this in detail in the next section. It is instructive to note at this point that this graphical technique is exactly equivalent to the partitioning idea of Kaplan et al. (1980).

III. THE SELF-CONSISTENT MEDIUM

The calculation of the self-consistent medium in the CCPA is of central interest and is the most important contribution of this work. To illustrate the procedure let us first consider a 2CPA. We shall indicate the generalization of bigger clusters subsequently.

Note first that after the delinking procedure according to the prescription described in the previous section, the resulting graph has the following structure: each bond in the original lattice has, in augmented space, an "octagon" decorating it (Fig.1a). The eight vertices of the octagon corresponds to the eight different configurations of the two-site cluster (2×2^2). Because of the cluster delinking, no octagon belonging to a bond has any connection to another, corresponding to another bond, through an augmented space link. This exactly implements the idea that within this approximation correlated scattering from three or more sites belonging to different bonds are ignored. The final effect is that each bond is renormalized as shown in Fig.1b. This gives rise to a matrix self-energy

$$\underset{\sim}{\Sigma} = \begin{pmatrix} \Sigma_0 & \Sigma_1 \\ \Sigma_1 & \Sigma_0 \end{pmatrix} .$$

The aim is to calculate $\underset{\sim}{\Sigma}$ self-consistently. It fully describes the self-consistent medium in the 2CPA.

The bond renormalization procedure follows in two steps:

(a) The decorating octagon is not an isolated octagon involving only the two spatial sites (0 and 1). If we look at the vertex A (i.e. $1f_1$ in the notation of Mookerjee 1973), the bond AE ($1f_1$ to $0f_1$) belonging to the octagon

is only one of the Z bonds emanating from A to the Z nearest neighbours of 1. The other remaining Z-1 bonds to $2f_1$, $3f_1$,... also hang on to the site A. Moreover these bonds themselves in turn have their own octagons decorating them (Fig.1c). Thus the bond AE is itself immersed in a self-consistent medium. The same is true for the bonds FG and HK of the octagon. We may take this into account by saying that the medium renormalizes the bonds AE, FG and HK. Once the renormalization is accounted for, the octagon is effectively isolated. The renormalized vertices $\sigma_0(z)$ and links $\sigma_1(z)$ are found as follows. Let us divide the lattice as follows into two subspaces (1) an unrenormalized bond AE, which we shall call system 1. It has a Hamiltonian $\underline{H}^{(1)} = V_2(\underline{T}_{AE} + \underline{T}_{EA})$. (2) A lattice L, which is the original lattice minus the link AE, and in which all bonds and sites are renormalized by $\underline{\Sigma}$. This has a Hamiltonian

$$\underline{H}^{(2)} = \Sigma_0(z) \sum_{i \neq A,E} \underline{P}_i + \Sigma_1(z) \sum_{i,j \neq A,E} \underline{T}_{ij} .$$

(3) A linking Hamiltonian

$$\underline{H}^{(int)} = \Sigma_1(z) \sum_{i} (\underline{T}_{iA} + \underline{T}_{Ai} + \underline{T}_{iE} + \underline{T}_{Ei}).$$

If we now use the notation $\underline{X}^{-P_y}$ to denote the inverse of the operator $\underline{X}$ in the subspace y

$$\underline{G}^{(1)} = \underline{P}_1 \underline{G} \underline{P}_1 = \left[z\underline{I} - \underline{H}^{(1)} - \underline{H}^{(int)} \underline{G}^{(2)} \underline{H}^{(int)} \right]^{-P_1} ,$$

$$\text{where } \underline{G}^{(2)} = \left[z\underline{I} - \underline{H}^{(2)} \right]^{-P_2}$$

$$\text{with } \underline{P}_1 + \underline{P}_2 = \underline{I} . \qquad (9)$$

Examination of the form of (9) immediately indicates that the effect of the rest of the lattice hanging on to the bond AE is to change the Hamiltonian $\underline{H}^{(1)}$ to $\underline{H}^{(1)} + \underline{\sigma}$ where the self-energy $\underline{\sigma}$ is given by

$$\sigma_{AA} = \sigma_{EE} = \sigma_0 = \Sigma_1^2(z) \sum_{k,m \in \mathcal{N}_A} G^{(2)}_{km}$$

$$\sigma_{AE} = \sigma_{EA} = \sigma_1 = \Sigma_1^2(z) \sum_{k \in \mathcal{N}_A} \sum_{m \in \mathcal{N}_E} G^{(2)}_{km} \qquad (10)$$

$\mathcal{N}_A$ denotes a nearest neighbour of A.

(b) Let us now work on the renormalized, isolated octagon. As before, let us divide the octagon into two subsystems: a bond B (0f,1f), the rest of the octagon M.

$$\underline{\tilde{H}}^{B} = \sum_{ij \in Of,1f} \underline{\tilde{H}}_{ij} \qquad \underline{\tilde{H}}^{M} = \sum_{ij \neq Of,1f} \underline{\tilde{H}}_{ij}$$

$$\underline{\tilde{H}}^{BM} = \sum_{i \in B} \sum_{j \in M} (\underline{\tilde{H}}_{ij} + \underline{\tilde{H}}_{ji}) \ .$$

As before, we have

$$\underline{G}^{B} = \underline{P}_{B}\, \underline{G}\, \underline{P}_{B} = \left[z\underline{I} - \underline{H}^{B} - \underline{H}^{BM}\, \underline{G}^{M}\, \underline{H}^{BM} \right]^{-1} \underline{P}_{B}$$

$$\underline{G}^{M} = \left[z\underline{I} - \underline{H}^{M} \right]^{-1} \underline{P}_{M} \ .$$

This immediately shows how the octagon renormalizes the bond B. We have

$$\Sigma_0 = H^{B}_{00} + \sum_{j \neq 0 \neq k} \sum H^{BM}_{0j}\, G^{M}_{jk}\, H^{BM}_{k0}$$

$$\Sigma_1 = H^{B}_{01} + \sum_{j \neq 0 \neq k \neq 1} \sum H^{BM}_{0j}\, G^{M}_{jk}\, H^{BM}_{k1} \ . \qquad (11)$$

Eqs.(10) and (11) together provide a self-consistent set of equations for the calculations of the self-energy $\underline{\Sigma}$. The various Green functions involved can be easily calculated on a three-dimensional lattice using the recursion technique of Haydock et al. In the case when we are using energy dependent effective Hamiltonians, the recursion has to be done separately for each value of energy.

The cluster generalization to arbitrary large clusters now follows exactly the same philosophy. Eqs.(10) and (11) remain the same. The only modification is the augmented space unit. For example, in the 3CPA the augmented space unit is the 24-gon (Fig.1d) (Mookerjee 1973) and

$$\underline{\Sigma} = \begin{bmatrix} \Sigma_0 & \Sigma_1 & \Sigma_1 \\ \Sigma_1 & \Sigma_0' & \Sigma_2 \\ \Sigma_1 & \Sigma_2 & \Sigma_0' \end{bmatrix} \ .$$

This has four independent components, but note that both (10) and (11) for this case also yield four equations:

$$\Sigma_0 = \Sigma_{AA} = H^{B}_{AA} + \sum_{k\ m} H^{BM}_{Ak}\, G^{M}_{km}\, H^{BM}_{mA}$$

$$\Sigma_0' = \Sigma_{BB} = H^{B}_{BB} + \sum_{k\ m} H^{BM}_{Bk}\, G^{M}_{km}\, H^{BM}_{mB}$$

$$\Sigma_1 = \Sigma_{AB} = H^{B}_{AB} + \sum_{k\ m} H^{BM}_{Ak}\, G^{M}_{km}\, H^{BM}_{mB}$$

$$\Sigma_2 = \Sigma_{BC} = H^{B}_{BC} + \sum_{k\ m} H^{BM}_{Bk}\, G^{M}_{km}\, H^{BM}_{mC} \ . \qquad (12)$$

We shall be interested in the diamond lattice, where the nearest neighbour cluster consists of 5 sites. Here the decorating lattice is a 160-gon (Mookerjee 1974) and the self energy is still four independent members

$$\underline{\Sigma} = \begin{bmatrix} \Sigma_0 & \Sigma_1 & \Sigma_1 & \Sigma_1 & \Sigma_1 \\ \Sigma_1 & \Sigma_0' & \Sigma_2 & \Sigma_2 & \Sigma_2 \\ \Sigma_1 & \Sigma_2 & \Sigma_0' & \Sigma_2 & \Sigma_2 \\ \Sigma_1 & \Sigma_2 & \Sigma_2 & \Sigma_0' & \Sigma_2 \\ \Sigma_1 & \Sigma_2 & \Sigma_2 & \Sigma_2 & \Sigma_0' \end{bmatrix} \ .$$

As the cluster size increases, the augmented space graph itself becomes large and the augmented space unit which renormalizes the cluster also becomes large. For clusters of size N, this unit is a $(N \times 2^{N})$-gon. However, the number of independent members in $\underline{\Sigma}$ still remains relatively small, and the $\underline{G}^{M}$ can be calculated by the recursion method with great facility even on quite large augmented space units. This fortunate marriage of the above method with the recursion technique reduces the calculation of quite large CCPAs to a tractable problem.

The self-consistent equations (10) and (11) involve an iterative solution for $\underline{\Sigma}$. We could, for example start with $\Sigma_0^0(z) = \Sigma_{CPA}$, $\Sigma_1^0(z) = V - i\delta$, use (10) to generate $\underline{\sigma}$, then (11) to get $\underline{\Sigma}^1$ and iterate the procedure. This method will be useful only if this procedure converges. The calculation was carried out on a bcc lattice with off-diagonal disorder. The procedure converged rapidly. Fig.2 shows the results. The most instructive feature is that the band width is larger than the 1CPA and clustering features appear in the minority region.

IV. RESULTS AND DISCUSSION

In this section we present results for single s-orbital per site model on a diamond lattice. To start with we have immersed a five-site cluster in a 1CPA medium. Consequently, the medium is not self-consistent. We therefore do not expect to get a good result near the band edges which are artifically

pushed to the 1CPA band edges with consequent distortion of the structure near them. Subsequently, we use the procedure described in the previous section to generate a self-consistent medium and immerse our five-site cluster in it. As expected the band edges move outwards and the details of the structure near the edges (particularly in the strong scattering impurity band case) is shown up with greater clarity (compare Figs.3 and 4).

Fig.4a shows results for the 50-50 alloy with small separation ($\delta = 0.5$) of the constituent atomic potentials. We first note that in three dimensions, in this "weak" scattering regime, clusters do not induce much structure. The bond and the site CPAs are virtually identical. Some structure is seen in the cluster CPAs and is in good agreement with the results of Mookerjee (1975b). Secondly, the density of states near the band centre actually increases as we go from the site to bond to cluster CPA, indicating that clusters inhibit band separation. For the 1CPA $\delta = 1$ is sufficient to separate the bands, while for the CCPA $\delta > 1$. This is also indicated by the moment method of Desjonqueres and Cyrot-Lackmann (1978) and the self-consistent boundary site approximation of Kumar and Joshi (1978).

Fig.4b shows a 50-50 alloy with a larger potential separation ($\delta = 1$). There is now greater structure in the CCPA results. The characteristic peak appears around $E \cong \pm 2.7$. The results are in good agreement with the earlier results of Mookerjee (1975) and the various boundary site approximation (Kumar, Kumar and Joshi 1975; Kumar and Joshi 1978). The self-consistent central-site approximation of Brouers et al. (1973) suffers from non-analyticity (violation of herglotzicity) at $E \cong 2.25$, leading to an unphysical discontinuity of the density of states at that energy. There is no separation of bands in the self-consistent CCPA.

Fig.4c shows a case of a 50-50 alloy with large separation ($\delta = 2$). Band separation is now unambiguous. The characteristic peak structure at $E \cong \pm 4.6$ and humps around $E = \pm 2.4$ and ± 5.5 are now prominent. As noted by Dean (1972) this central peak is due to states localized on isolated B atoms and the two satellite humps due to states localized on bonding and antibonding states on AB pairs. Note however that the effect of these structures are far less prominent in three than in one dimensional systems. The results are in good agreement with the boundary site results.

Fig.4d shows the case of a 90-10 alloy with large separation ($\delta = 1$). This is what is often referred to as the strong scattering regime. The majority band is almost like the pure host with the twin peaks of the diamond structure. The van Hove singularities, however, have been considerably smoothened out. The impurity band shows considerable structure. The three peaked structure is

now even more prominent. Again the results are in good agreement with moments and boundary site approximations.

For larger separations the boundary site approximations start to show violation of herglotzicity. For $\delta = 2$, for example, around $E = 3.2$ and between $E = 3.46$ and 3.48 branch cuts appear off the real energy axis. This immediately restricts the use of these approximations precisely in those regimes of strong scattering where clustering structure is most prominent. However, because of the graphical methodology and recursion techniques used in our work, herglotz behaviour is assured for all energies and all ranges of disorder.

In Figs.4a-d, the effects of short-range ordering is also displayed. The effect is throughout consistent and helps us to distinguish the origin of various peaks. $\alpha < 1$ increases the probability of unlike or AB configurations. This decreases the central peak, which is related to isolated B or BBBBB clusters. Whereas $\alpha > 1$ increases the probability of precipitating B clusters in a A medium thus greatly enhancing the central peak. The reverse effect is seen on the satellite peaks. The 90-10 impurity band shows the greatest effect of short-range ordering, again consistent with the above interpretation.

These preliminary calculations on a simple model are encouraging and provide us with sufficient theoretical basis to apply this method to the more realistic situations of the III-V alloys.

ACKNOWLEDGMENTS

Two of the authors (V.K.) and (A.M.) would like to thank Professor Abdus Salam, the International Atomic Energy Agency and UNESCO for hospitality at the International Centre for Theoretical Physics, Trieste.

REFERENCES

Anderson, P.W. (1969) Phys. Rev. 181, 25.

Bishop, A.R. and Mookerjee, A. (1974) J. Phys. C 7, 2161.

Brouers, F., Ducastelle, F., Gautier, F. and Van der Rest, J. (1973) J. Phys. F 3, 2120.

Bullett, D.W. (1975) J. Phys. C 8, 2695.

Dean, P. (1972) Rev. Mod. Phys. 44, 127.

Desjonqueres, M.C. and Cyrot-Lackmann, F. (1978) J. Phys. F 7, 61.

Diehl, H.W. and Leath, P.L. (1979a) Phys. Rev. B19, 596; (1979b) Phys. Rev. B19, 879.

Haydock, R. (1972) Thesis (University of Cambridge).

Haydock, R., Heine, V. and Kelly, M.J. (1972) J. Phys. C 5, 2845.

Kaplan, T. and Gray, L.J. (1976) Phys. Rev. B14, 3462; (1977) Phys. Rev. B15, 3260.

Kaplan, T., Leath, P.L., Gray, L.J. and Diehl, H.W. (1980) Phys. Rev. B21, 4230.

Kumar, V., Kumar, D. and Joshi, S.K. (1975) Phys. Rev. B11, 2831.

Kumar, V. and Joshi, S.K. (1978) Phys. Rev. B18, 2515.

Kumar, V. and Joshi, S.K. (1979) Ind. J. Phys. (Commemoration Vol.2), 1.

Mookerjee, A. (1973) J. Phys. C 6, 1340; (1975a) J. Phys. C 8, 1524; (1975b) J. Phys. C 8, 29; (1979) Disorder Systems (Monograph: Hindustan Publishing Corporation).

Mookerjee, A. and Chaudhry, V. (1980) ICTP, Trieste, preprint IC/80/143.

FIGURE CAPTIONS

Fig.1 a) The augmented space octagon decorating a bond.
b) Renormalization of the bonds by augmented space octagons.
c) Renormalization of the octagon by the medium.
d) The augmented space 24-gon for a 3CPA calculation.

Fig.2 Self energies in the 1CPA and 2CPA calculations.

Fig.3 Impurity band of a 90-10 alloy with $\delta = 1$ in the CCPA with 1CPA medium and the self-consistent CCPA medium.

Fig.4 a) 50-50 alloy with $\delta = 0.5$.
b) 50-50 alloy with $\delta = 1$.
c) 50-50 alloy with $\delta = 2$.
d) 90-10 alloy with $\delta = 1$.

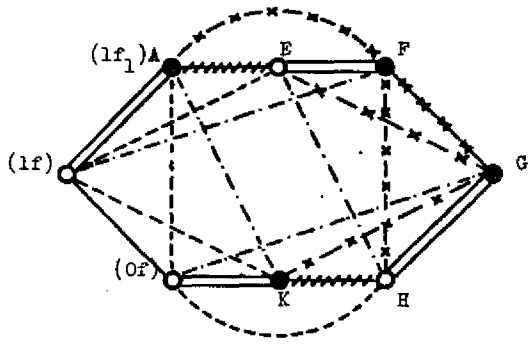

DICTIONARY

$V_1 = 2c\phi_2 + c^2\phi_1 + V_{BB}$

$V_2 = \phi_2 + c(1-c)\phi_1 + V_{BB}$

$V_3 = 2(1-c)\phi_2 + (1-c)^2\phi_1 + V_{BB}$

$= \sqrt{c(1-c)}\ (\phi_2 + (1-c)\phi_1$

$= \sqrt{c(1-c)}\ (\phi_2 + c\phi_1)$

$= c(1-c)\phi_1$

$= \Sigma\, c(1-c)$

$= e_B + cE$

$= e_B + (1-c)E$

FIG 1 (a)

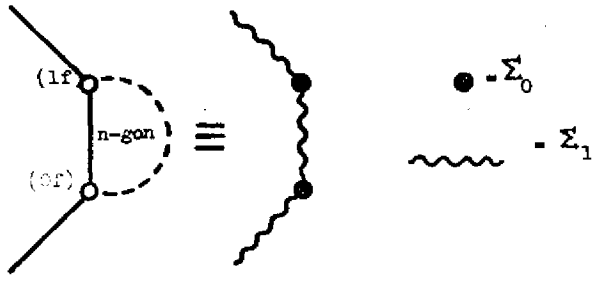

FIG 1 (b)

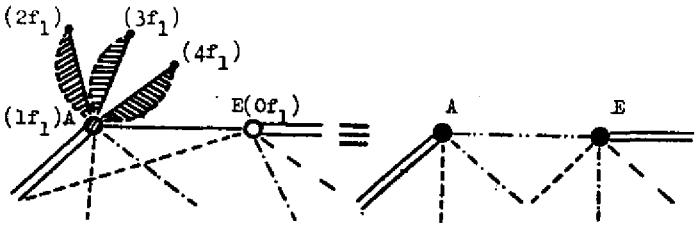

represents an octagonal decoration as in Fig 1a.

● - σ_0

—·—·— - σ_1

FIG 1 (c)

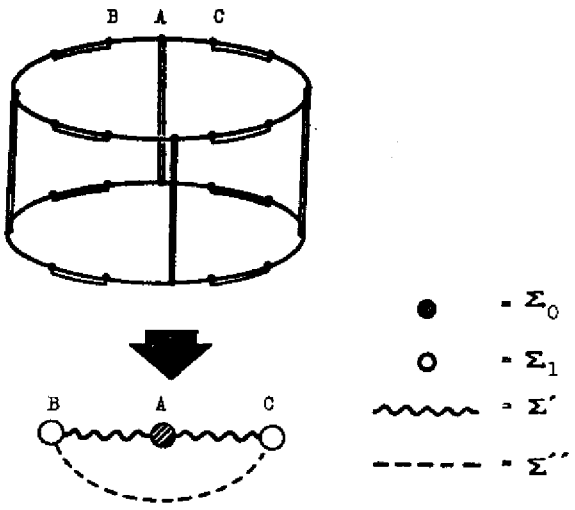

FIG 1 (d)

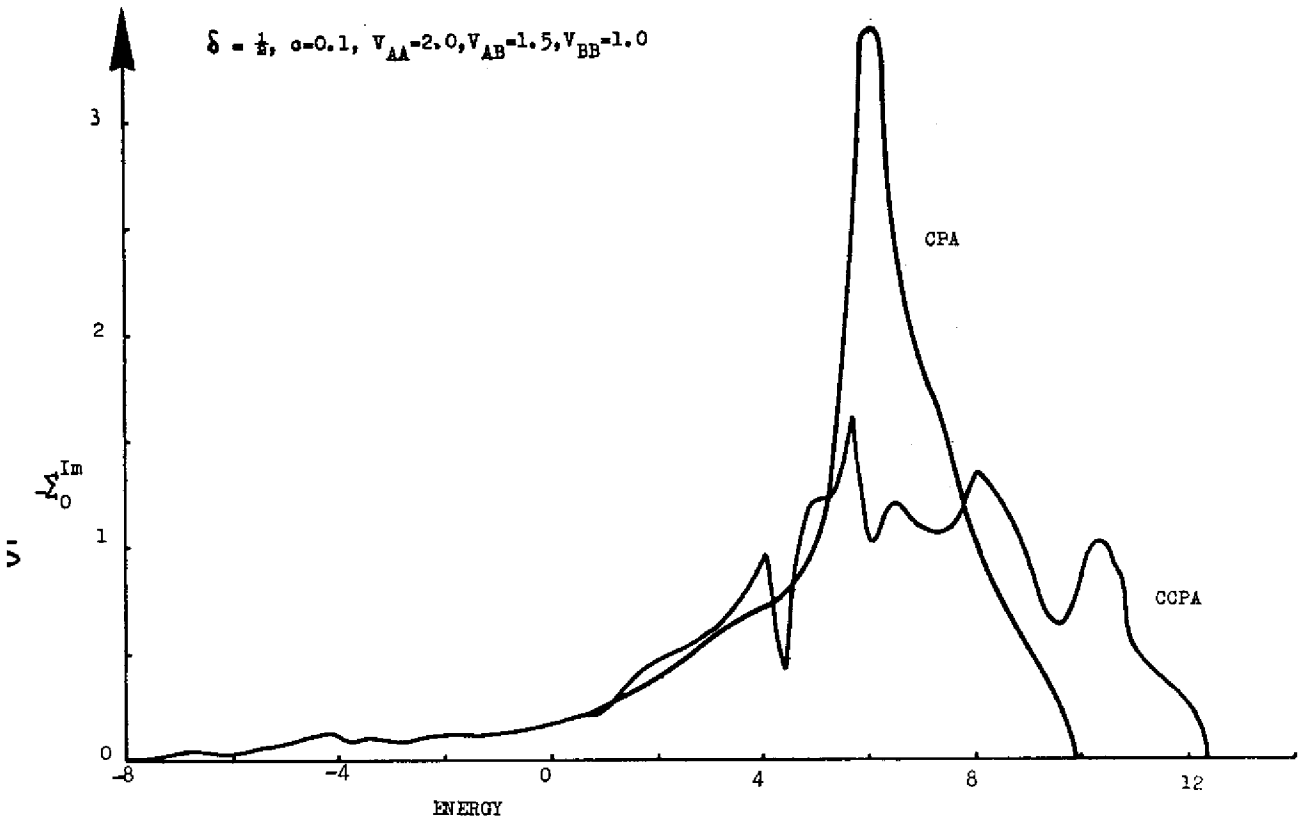
δ = ½, c=0.1, V_{AA}=2.0, V_{AB}=1.5, V_{BB}=1.0
CPA
CCPA
$-\Sigma_0^{Im}$
ENERGY

FIG 2 (a)

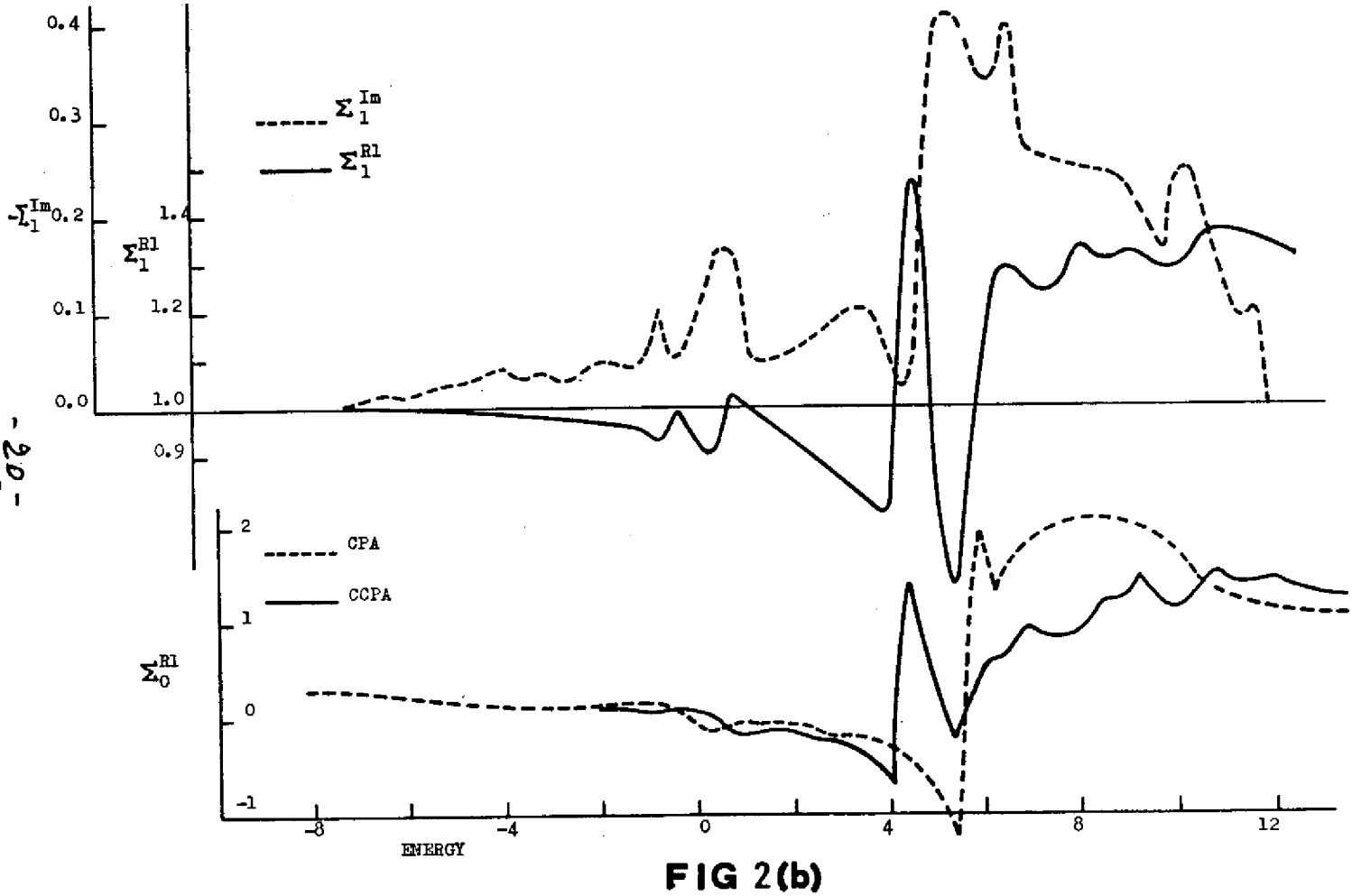
Σ_1^{Im}
Σ_1^{Rl}
$-\Sigma_1^{Im}$
Σ_1^{Rl}
CPA
CCPA
Σ_0^{Rl}
ENERGY

FIG 2(b)

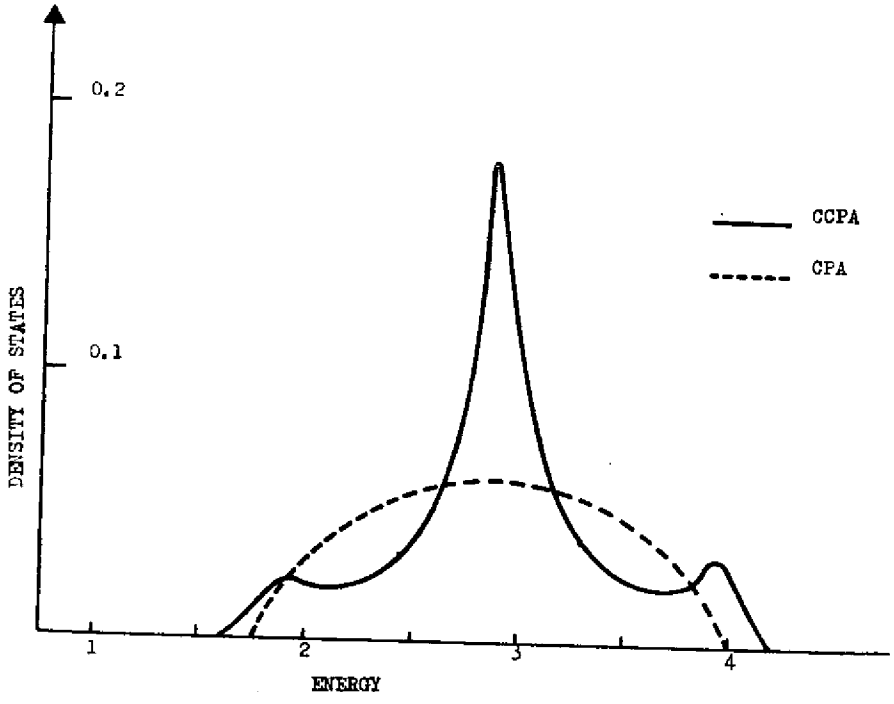
0.2
0.1
DENSITY OF STATES
CCPA
CPA
1
2
3
4
ENERGY

FIG 3

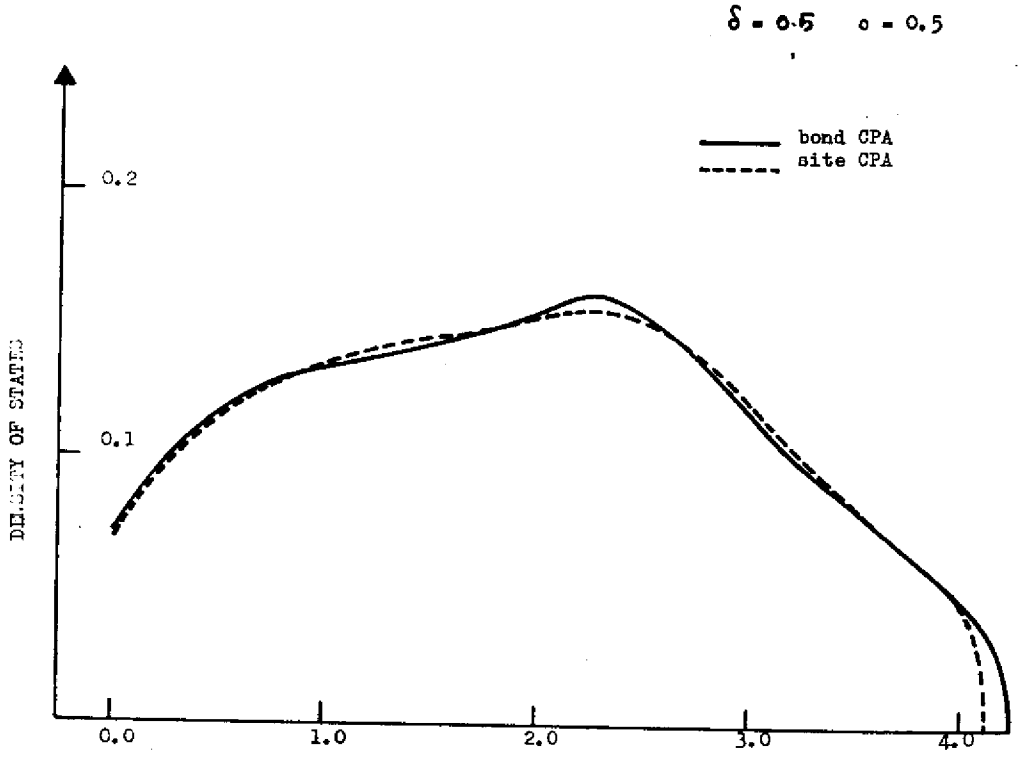
δ = 0.5 c = 0.5
bond CPA
site CPA
0.2
0.1
0.0
1.0
2.0
3.0
4.0

FIG 4a(i)

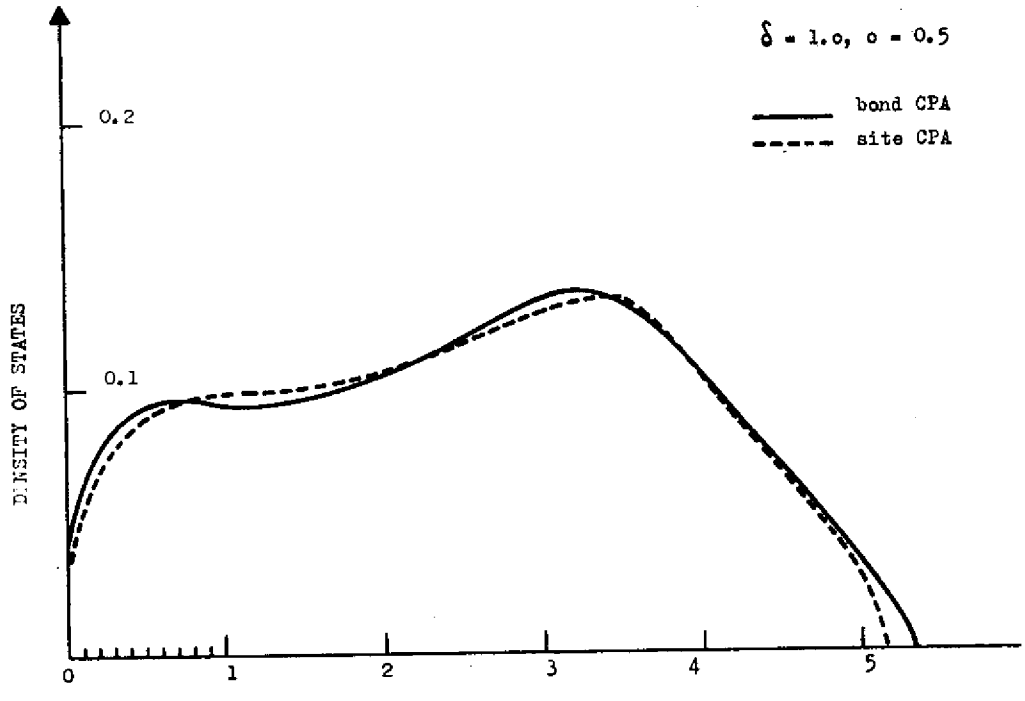

FIG 4b(i)

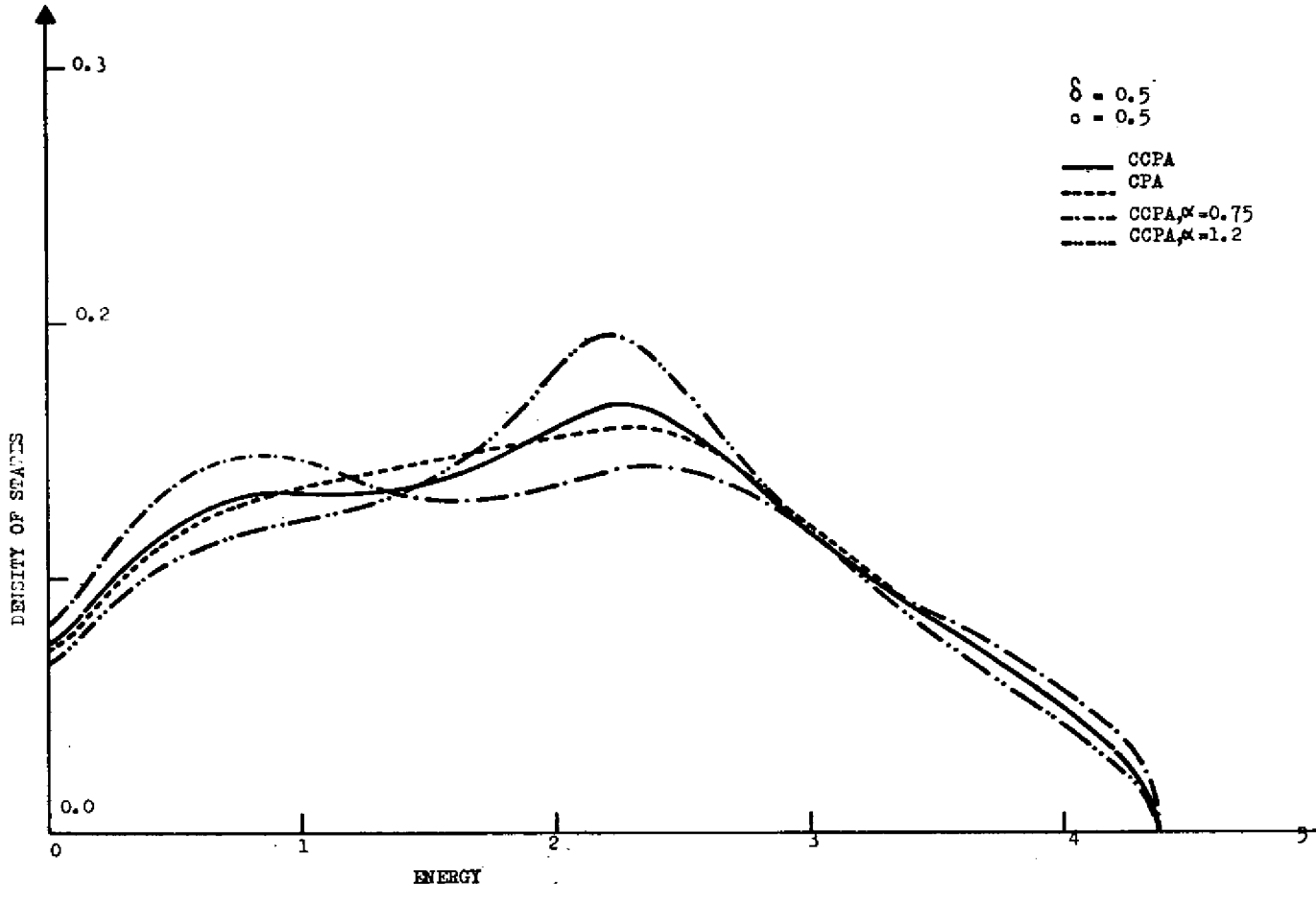

FIG 4a (ii)

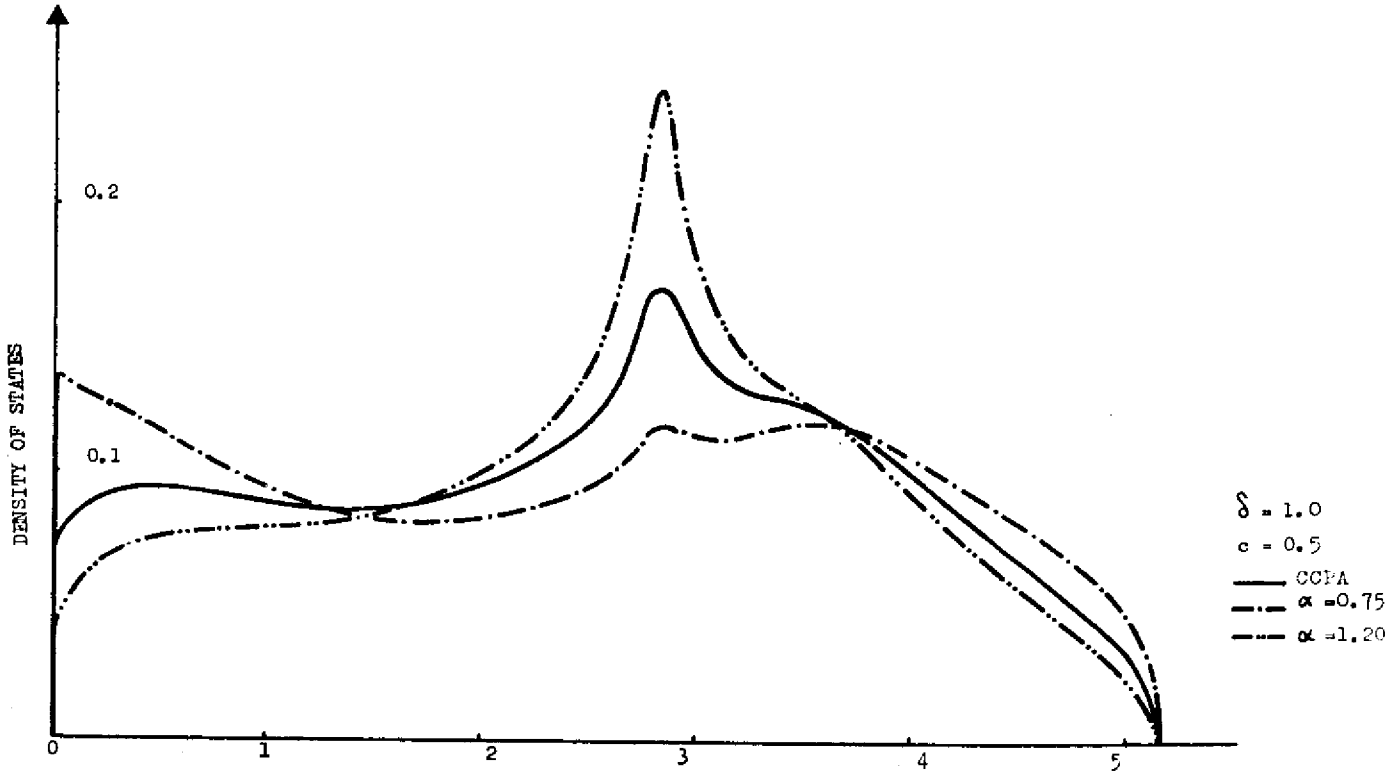

FIG 4b (ii)

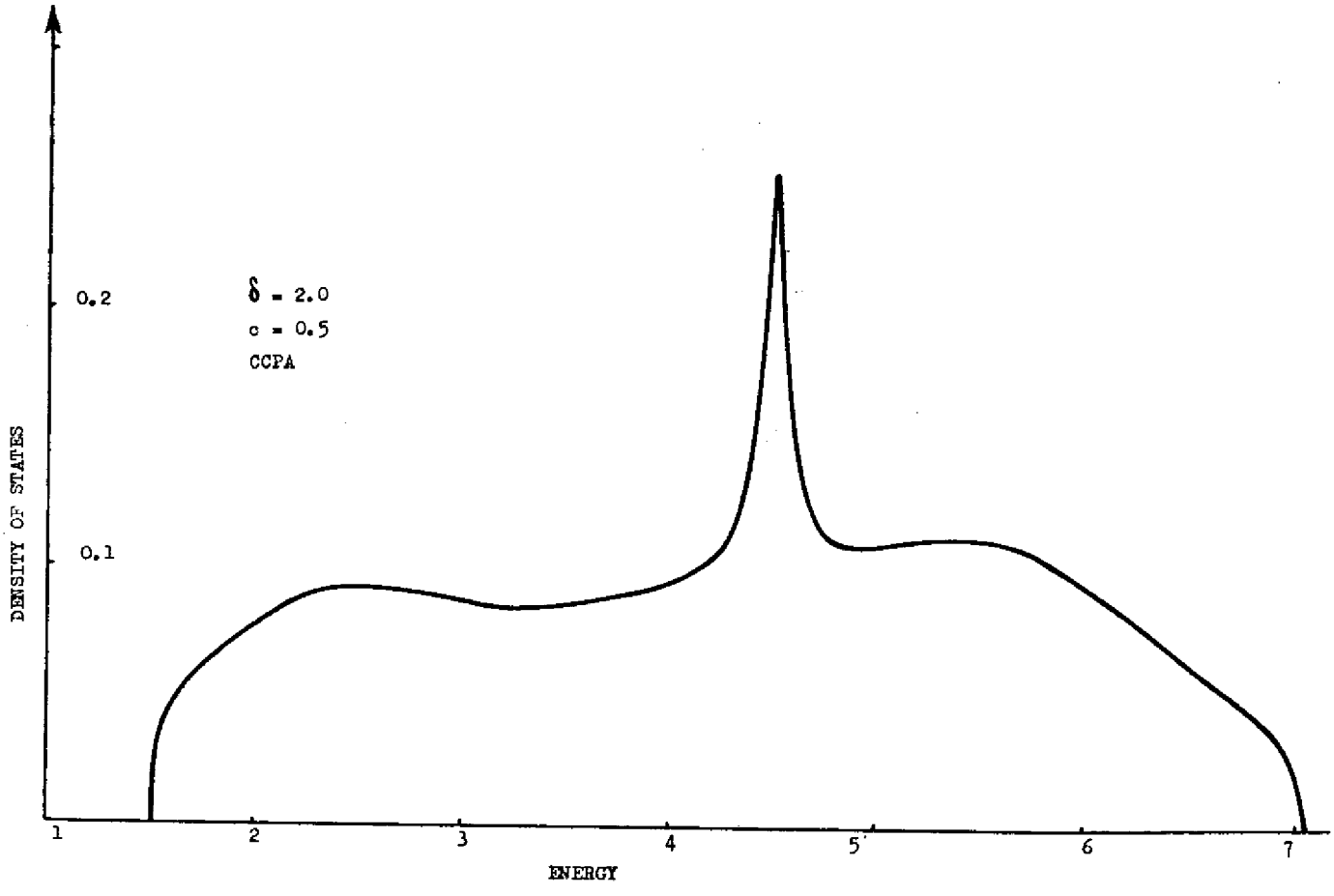

FIG 4 (c)

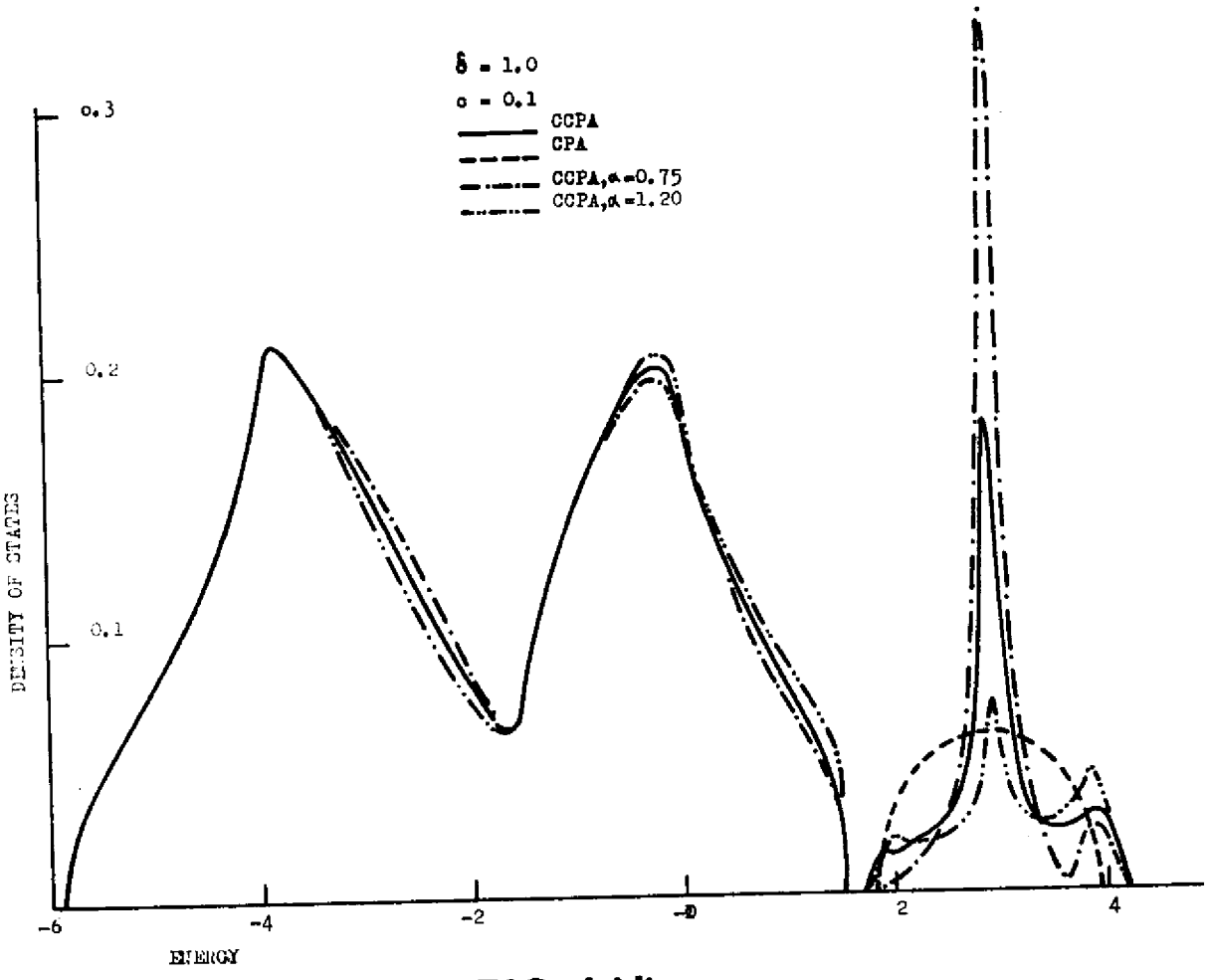
δ = 1.0
c = 0.1
CCPA
CPA
CCPA,α=0.75
CCPA,α=1.20
0.3
0.2
0.1
DENSITY OF STATES
-6
-4
-2
-0
2
4
ENERGY

FIG 4 (d)

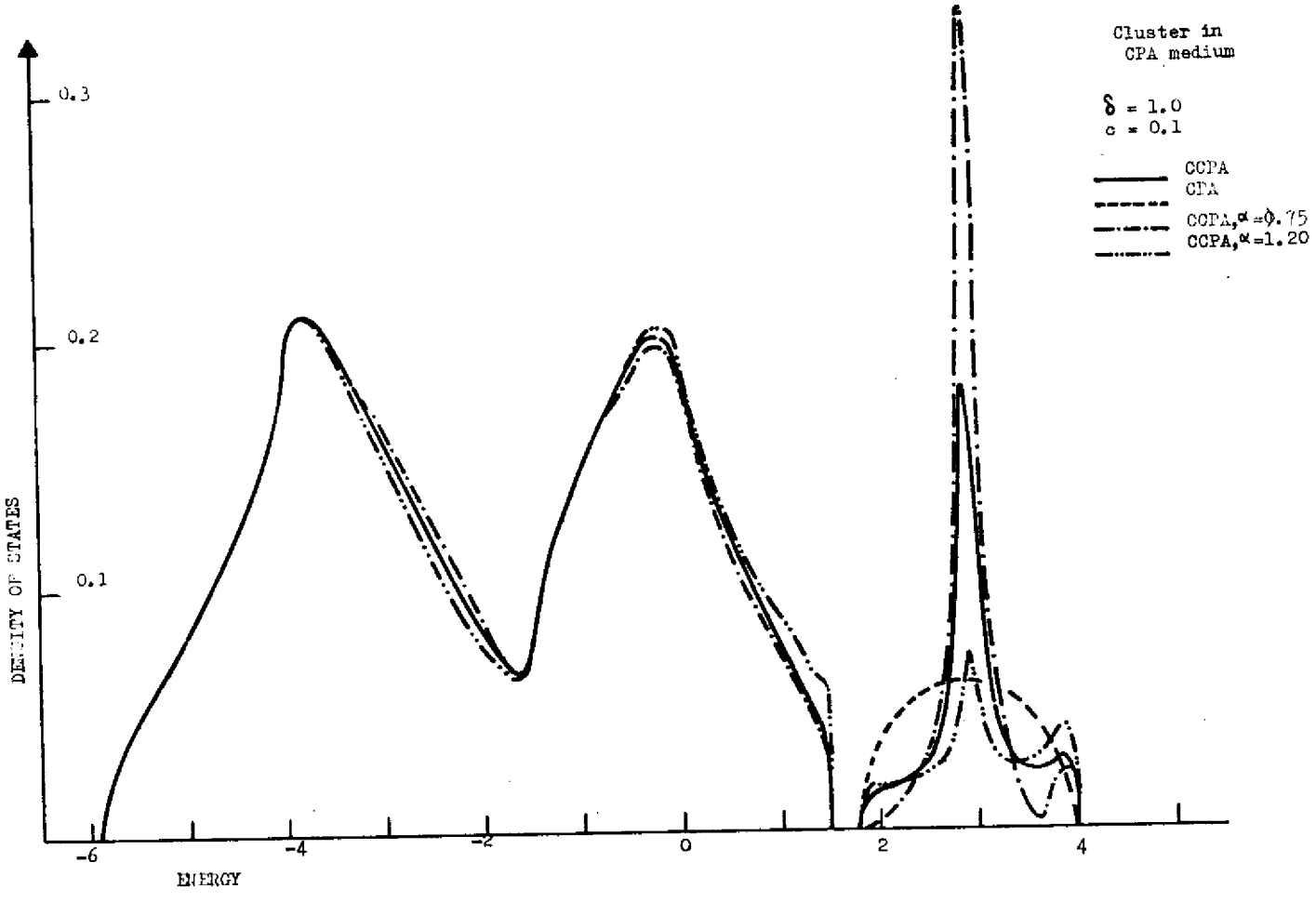
Cluster in
CPA medium
δ = 1.0
c = 0.1
CCPA
CPA
CCPA,α=0.75
CCPA,α=1.20
0.3
0.2
0.1
DENSITY OF STATES
-6
-4
-2
0
2
4
ENERGY

FIG 5